Biochimica et Biophysica Acta 1797 (2010) 250–254

Contents lists available at ScienceDirect

Biochimica et Biophysica Acta

journal homepage: www.elsevier.com/locate/bbabio

A quantum mechanics/molecular mechanics study of the tyrosine residue, Tyr_D, of Photosystem II

Richard Hart, Patrick J. O'Malley *

School of Chemistry, The University of Manchester, Oxford Road, Manchester, M13 9PL, UK

ARTICLE INFO

Article history:
Received 25 August 2009
Received in revised form 23 October 2009
Accepted 27 October 2009
Available online 3 November 2009

Keywords:
Photosystem II
Oxygen Evolving Complex
Tyrosine radical
B3LYP
Electron Transfer

ABSTRACT

QM/MM calculations have been used to monitor the oxidation of the D2-Tyr160, Tyr_D, residue involved in redox reactions in Photosystem II. The results indicate that in the reduced form the residue is involved in hydrogen bond donation via its phenolic head group to the τ-nitrogen of the neighboring D2-His189 residue. Oxidation to form the radical is accompanied by spontaneous transfer of the phenolic hydrogen to the τ-nitrogen of D2-His189 leading to the formation of a tyrosyl-imidazolium ion complex. Deprotonation of the imidazolium ion leads to the formation of a tyrosyl-imidazole neutral hydrogen-bonded complex. Comparison of calculated and experimental hyperfine coupling tensors and *g*-tensors suggests that the neutral imidazole complex is formed at physiological temperatures while the imidazolium complex may be stabilized at cryogenic temperatures.

1. Introduction

In plant, algae and cyanobacterial photosynthesis, Photosystem II (PS II) drives the light-induced reduction of plasoquinone to plastoquinol resulting in the oxidation of water to oxygen[1–3] Two tyrosine residues of the PS II complex, D2-Tyr160 (Tyr_D) and D1-Tyr161 (Tyr_Z) are redox active[4–6]. Tyr_Z forms a transient radical and is believed to be directly involved in the electron-transfer reactions leading to oxygen evolution. X-ray crystallography has shown [7] that it is situated directly between the primary donor P680 and the CaMn4 oxo complex which catalyses the oxidation of two water molecules to a molecule of oxygen and four protons (Fig 1).

Oxidation of Tyr_D, by contrast, forms a neutral tyrosine radical which is stable in the dark and whose function is not fully understood [5]. It is part of the D2 protein and is not in the direct pathway of electron transfer from the oxidized water molecules. Because of its stability, the Tyr_D radical has been well characterized by magnetic resonance and FTIR methods [8–11]. From the crystal structure, D2-His189 is within hydrogen bond acceptor distance to the reduced Tyr_D via its τ-nitrogen atom [7] On oxidation of Tyr_D, it has been proposed that the phenolic proton is transferred to the imidazole group of this histidine. The transferred proton then hydrogen-bonds back to the tyrosine radical oxygen with possible subsequent deprotonation of the imidazole at the π-nitrogen atom [12,13]. These proposed events have received support from small model gas-phase electronic structure calculations on phenoxyl-imidazole models [14–16]. So far, however, no computational approach has taken account of the immediate protein environment surrounding Tyr_D as revealed by X-ray crystallography [7].

In this study, therefore, we use quantum mechanics/molecular mechanics, QM/MM, calculations to model the effect of the immediate protein environment on electron and proton transfers occurring on Tyr_D oxidation. In such a fashion the redox species is constrained to its position and relative orientation as determined by the X-ray crystal structure determination and the influence of neighboring amino acid residues on geometries, proton transfer and spin density distribution can be accounted for. The models are validated by calculation of hyperfine couplings and *g*-tensor values for comparison with experimental determinations via EPR methods.

The Tyr_D free radical is somewhat unique in being essentially fully characterized experimentally by EPR techniques, with a full range of ^{13}C, ^{1}H, ^{15}N and ^{17}O hyperfine tensor measurements available in addition to the *g*-tensor principal values [8,17–23]. Such extensive magnetic resonance information concerning an *in vivo* biologically significant free radical is unprecedented and provides a stringent test of modeling methods based on QM/MM to calculate experimental EPR parameters for a biological free radical *in situ*.

2. Methods

To prepare our models for QM/MM studies the initial heavy atom coordinates were extracted from the most highly resolved Photosystem II crystal structure determination, 2AXT [7]. All amino acids

Abbreviations: DFT, density functional theory; B3LYP, Becke3 Lee Yang Parr; EPR, electron paramagnetic resonance; ENDOR, electron nuclear double resonance; QM/MM, quantum mechanics/molecular mechanics; ONIOM, Own N-Layer Integrated molecular Orbital molecular Mechanics; ME, Mechanical embedding; EE, Electrostatic embedding

* Corresponding author. Tel./fax: +41612004536.
E-mail address: patrick.omalley@manchester.ac.uk (P.J. O'Malley).

0005-2728/$ – see front matter © 2009 Elsevier B.V. All rights reserved.
doi:10.1016/j.bbabio.2009.10.010

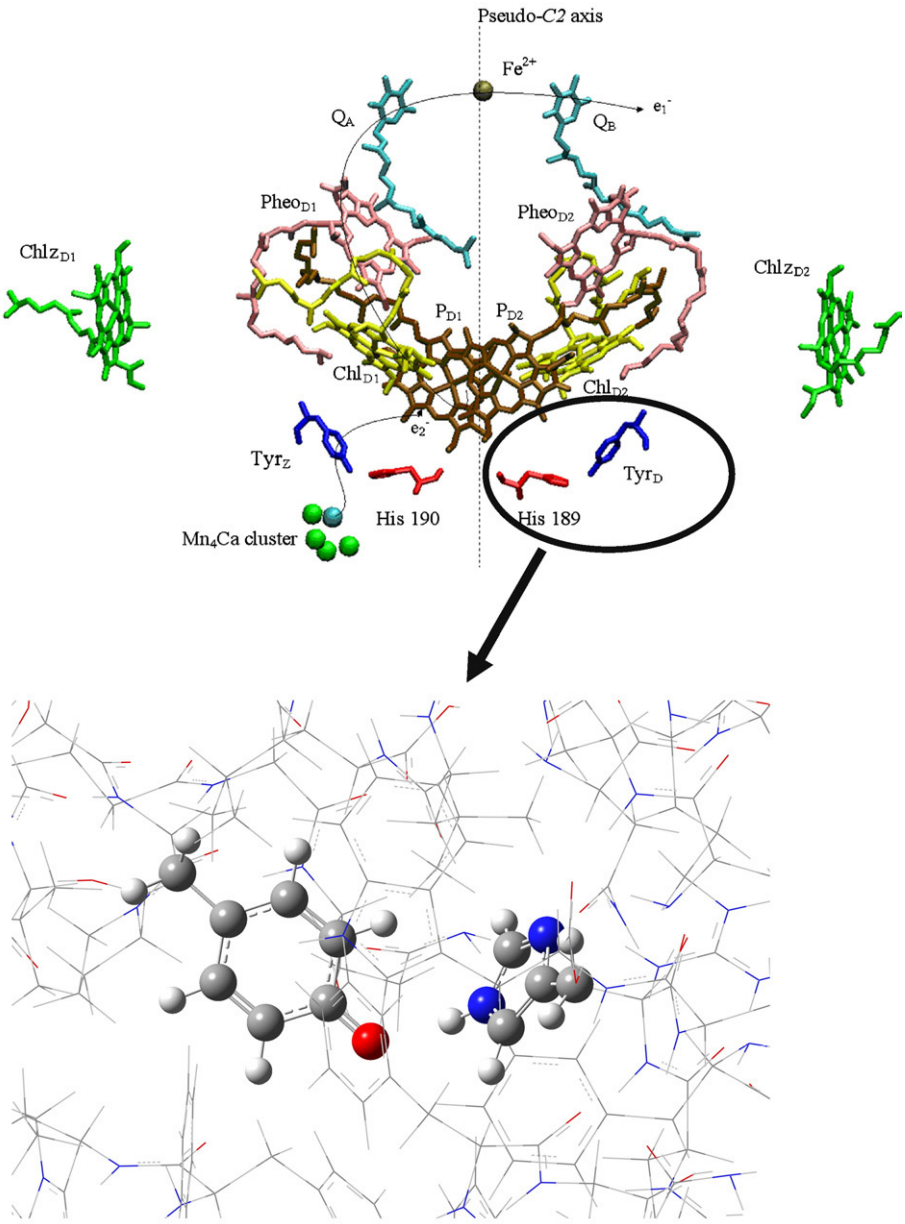

Fig. 1. Electron transfer components of Photosystem II indicating direction of electron flow from water to plastoquinones Q_A and Q_B. Expansion demonstrates Tyr_D local environment. For calculation purposes all atoms in ball and stick representation were assigned to the QM layer with surrounding atoms assigned to the MM layer, see text for calculation details.

within 10 Å of the Tyr_D phenol-ring oxygen atom were included. Hydrogen atoms were added using standard geometries as determined by the program Gaussview [24]. QM/MM calculations were then carried out on this model with the atoms of the Tyr_D and D2-His189 being included in the QM layer and all other atoms were included in a second layer using the United Atom Forcefield (UFF); see Fig 1 for a demonstration of the partitioning scheme used. For the QM/MM studies the ONIOM method was employed [25]. Both mechanical embedding (ME) and electrostatic embedding (EE) QM/MM schemes were used as implemented in the electronic structure program Gaussian 03 [24,25]. Geometry optimization of the QM atoms was performed at the ONIOM (UB3LYP/6–31G(d,p):UFF) level. For the free radical forms single point calculations at the ONIOM (UB3LYP/EPR-II//UB3LYP/6–31G(d,p):UFF) were then carried out to obtain hyperfine couplings and *g*-tensor values. For the *g*-tensor calculation the Gauge Independent Atomic Orbital (GIAO) method as implemented in Gaussian 03 was used. As a test of our methodology we also carried out calculations using the PBE0 functional instead of B3LYP. This function has been shown before to perform similarly to B3LYP for free radical hyperfine couplings and this is confirmed in our studies on this system. As most of the previous studies for smaller models have been performed using the B3LYP functional, thereby permitting direct comparison with our data for the extended system here, we present the B3LYP values for discussion only.

3. Results and discussion

Initially the reduced system was geometry optimized and the principal bond distances are given in Fig. 2. In the reduced system the calculations show that the phenolic hydrogen is retained on the Tyr_D i.e. no deprotonation is predicted to occur from the phenolic OH group to the neighboring D2-His189 in the reduced state. The phenolic hydrogen is involved in hydrogen bond donation to the τ-nitrogen of the imidazole group of D2-His189. The relevant optimized bond distances are given in Fig. 2. Optimization on radical formation results in a transfer of the phenolic proton to the τ-nitrogen atom of D2-

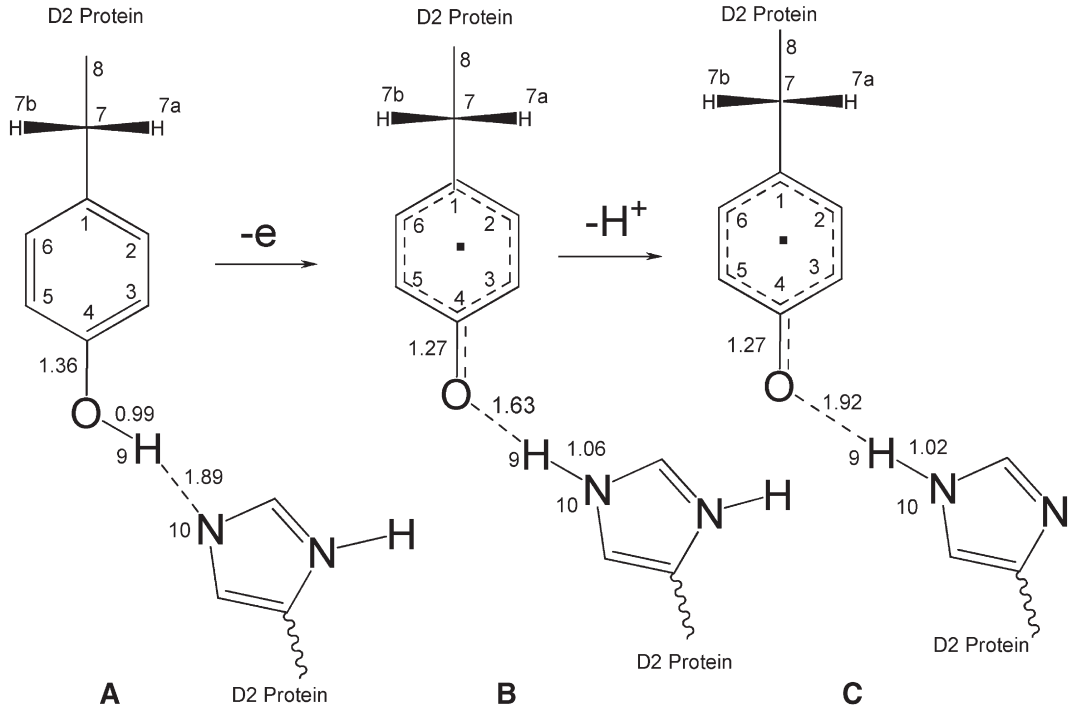

Fig. 2. Schematic representation of events accompanying Tyr_D oxidation in Photosystem II. (A) reduced form. (B) tyr-imidazolium ion complex, (C) tyr-imidazole complex. Labeling of atoms used throughout is illustrated. Bond distances are given in angstroms.

His189 which then forms a hydrogen bond with the oxygen atom of the resultant Tyr_D radical. This results in an imidazolium ion formation on D2-His189. Deprotonation of D2-His189 via its π-nitrogen leads to a neutral imidazole-tyrosine radical hydrogen bonded complex which was then further optimized. The principal optimized bond distances for these two radical models are given also in Fig. 2. For the neutral imidazole radical the hydrogen bonding distance is increased compared with the charged imidazolum form suggesting a decrease in hydrogen bonding interaction compared with the charged model.

The full ^{13}C, ^{1}H, ^{15}N and ^{17}O tensors for both imidazolium and imidazole models have been calculated using both QM/MM-ME and QM/MM-EE schemes. Both embedding methods lead to very similar results and for discussion purposes only the ME data are included here. The QM/MM-ME calculated hyperfine coupling tensors are given in Tables 1 and 2 for both the charged and neutral forms together with experimental determinations. Taking the ^{13}C data for comparison initially, it can be seen (Table 1) that both imidazolium and imidazole forms give highly satisfactory agreement with experiment considering the experimental error estimate in the measurement of these hyperfine couplings is 0.7 G [17]. A notable exception to this trend is the minor tensor components for the three and five positions where the magnitude of the experimental components is far greater than the predicted values (Table 1). We attribute the difference here to errors in the reported experimental values. The small calculated values would be essentially impossible to measure using the experimental approaches used. For phenoxyl free radicals in solution the 3/5 ^{13}C isotropic hyperfine coupling has been reported to be 8.1 G [14] which is in poor agreement with the experimental ^{13}C value for the C5 position of 4.3 G but in general accord with the calculated values for the charged and deprotonated model calculated values of 6.3 and 7.2 G respectively. A more extensive discussion of these hyperfine couplings can be found in [14]. For all other positions the agreement between experimental and calculated values is very satisfactory. Based on the comparison between the neutral and charged model it is difficult to differentiate based on the ^{13}C data alone.

Moving on to the ^{1}H data (Table 2), the agreement with experimental and calculated values is again good. Of particular note here is the good agreement observed for the 7a and 7b protons of the tyrosyl methylene group. As has been well documented for various tyrosyl free radicals these protons receive spin density via hyperconjugation with the ring centered C1 π-spin density and their values

Table 1
^{13}C and ^{17}O Hyperfine (isotropic plus anisotropic) coupling tensors calculated at the ONIOM (UB3LYP/EPR-II//UB3LYP/6–31G(d,p):UFF) level for imidazolium and imidazole forms of the Tyr_D radical compared with experimental determinations [17, 21] and in brackets values for a smaller cluster imidazolium model from [14] are also given for comparison.

	Experimental	Calculated	
	A_{11} A_{22} A_{33}	Imidazolium A_{11} A_{22} A_{33}	Imidazole A_{11} A_{22} A_{33}
C1	2.0	2.0 (0.3)	2.4
	2.0	2.4 (0.8)	2.9
	34.5	34.2 (35.4)	34.2
C2	−12.5	−10.9 (−12.8)	−14.1
	−7.5	−6.1 (−6.2)	−6.4
	−5.0	−5.5 (−5.6)	−5.8
C3	−5.0	−0.9 (−0.9)	−0.2
	−5.0	−0.5 (−0.4)	0.3
	19.0	16.1 (20.4)	19.8
C4	−11.0	−10.2 (−10.5)	−12.8
	−10.0	−8.6 (−8.8)	−11.5
	−8.0	−6.6 (−7.0)	−9.4
C5	−4.0	−0.7 (−0.7)	−0.2
	−4.0	−0.2 (−0.3)	0.2
	21.0	19.7 (20.6)	21.7
C6	−12.5	−13.8 (−13.6)	−14.3
	−7.5	−6.4 (−6.1)	−6.7
	−5.0	−5.8 (−5.5)	−6.1
O4	6.0	9.1 (8.1)	11.2
	6.0	9.0 (7.8)	11.1
	−43.5	−44.9 (−43.4)	−49.9

All hyperfine coupling constants are given in Gauss (G).

Table 2
^{1}H and ^{14}N Hyperfine (isotropic plus anisotropic) coupling tensors calculated at the ONIOM (UB3LYP/EPR-II//UB3LYP/6–31G(d,p):UFF) level for imidazolium and imidazole forms of the Tyr_D radical compared with experimental determinations [8, 12, 23] and in brackets values for a smaller cluster imidazolium model from [14] are also given for comparison.

	Experimental	Calculated	
	A_{11} A_{22} A_{33}	Imidazolium A_{11} A_{22} A_{33}	Imidazole A_{11} A_{22} A_{33}
H2	–	0.4 (1.2)	1.3
	1.6	1.3 (1.9)	2.1
	2.6	2.6 (3.2)	3.7
H3	−9.1	−8.1 (−9.8)	−9.3
	−6.9	−6.2 (−7.3)	−7.2
	−2.9	−1.7 (−2.5)	−2.4
H5	−9.8	−9.5 (−9.9)	−10.1
	−7.3	−7.3 (−7.6)	−7.7
	−2.9	−2.3 (−2.6)	−2.6
H6	–	1.1 (1.2)	1.4
	1.6	2.0 (2.1)	2.2
	2.6	3.3 (3.5)	3.7
H7b	3.3–4.1	3.9	3.5
	1.4–2.3	2.2	1.8
	1.4–2.3	1.9	1.6
H7a	10.4–11.8	13.9	12.6
	8.7–10.2	12.0	10.8
	8.7–10.2	11.5	10.4
Nτ	0.2	−0.5 (−0.4)	−0.2
	0.2	−0.4 (−0.4)	−0.2
	0.2	−0.3 (−0.3)	−0.1
H8	–	3.4 (2.8)	2.8
	−1.3	−2.2 (−1.2)	−1.3
	−1.3	−2.0 (−1.4)	−1.2

All hyperfine coupling constants are given in Gauss (G).

vary depending on the extent of overlap with this spin density [14]. The extent of this overlap and hence the ensuing hyperfine coupling depends on the C8–C7–C1–C2 dihedral angle. From the crystal structure determination [7], 2AXT, this dihedral angle value is 122°. In this QM/MM study the dihedral angles are optimized under the constraint of the surrounding protein environment and in the optimized geometries for the imidazolium and imidazole models, this value changes to 108° and 109° respectively. In the EPR literature on this topic the "dihedral angles" usually discussed are the ones between the H7 protons and the "p_z" orbital on C1 assuming ideal tetrahedral geometry. This is depicted in Fig. 3. Enantiomeric substitution plus EPR studies have been used to determine the absolute configuration for this group [18]. The calculated values of this study are compared with these experimental determinations in Fig. 3 where we show that the calculated values are within the experimental error determination for both imidazolium and imidazole forms. As shown in [8] the value of these hyperfine couplings can vary slightly depending on the species studied. Our calculated hyperfine coupling values in Table 2 are in good agreement with this range again suggesting that the conformation of the free radical in the protein environment is well reproduced by our QM/MM optimizations.

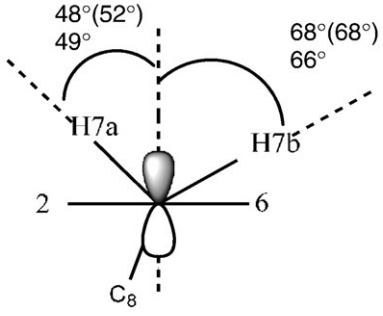

Fig. 3. Comparison of calculated and experimentally derived orientations (dihedrals, see text) for the Tyr_D methylene group hydrogens. Values shown are for the imidazole (top) and imidazolium (bottom) forms. The experimentally derived values from [18] are given in brackets.

The calculated ^{17}O hyperfine coupling tensor (Table 1) is also in good agreement with the experimental determinations [17,22]. The agreement appears best with the charged imidazolium form. It has however, been noted previously from studies of semiquinone free radicals[26] that calculations at this level tend to overestimate ^{17}O hyperfine couplings by 4–5%, so again it is difficult to distinguish between the two models.

The hyperfine couplings from the hydrogen bonded proton H8 and the τ-nitrogen atom are crucial to investigate the nature of hydrogen bonding between the Tyr_D free radical and the D2-His189 residue [27]. Table 2 indicates that both of these hyperfine coupling data sets are better reproduced by the neutral imidazole model. The magnitude of the calculated values for the imidazolium model is around twice the experimentally determined values. Much better agreement is therefore found for the imidazole model. As these data are the most direct monitors of the hydrogen bond interaction they suggest that the form observed experimentally at physiological temperatures is the imidazole model.

Tables 1 and 2 also compare calculated hyperfine couplings from a previous study on an isolated cluster small model. While care must be exercised, as the optimization procedures are different for each study, there are no major changes in the magnitudes of the hyperfine couplings brought about by inclusion of the surrounding protein environment model. For the smaller model the analysis of the methylene protons described above cannot be carried out of course as the methylene 7a and 7b protons are modeled by a methyl group. In a recent ENDOR study of the Tyr_D radical on single crystals [28] it was possible to distinguish the H5/H3 hyperfine couplings and assign the larger value to the H5 position. This small and subtle difference is faithfully reproduced by our calculated values in Table 2 for both the imidazole and imidazolium forms. In the experimental study very small differences in the values for the H2 and H6 proton hyperfine couplings were also proposed with the larger couplings being assigned to the two positions. For the imidazole model essentially identical couplings are predicted for both positions (Table 2), whereas the imidazolium model predicts larger values for the H6 position. Due to the minute difference attributed in the experimental analysis and the complex spin polarization scheme for this position [14] it is not realistic to expect the model to reproduce such tiny effects.

In addition we have calculated the *g*-tensors for both free radical models. For the imidazole model, the values are $g_{xx} = 2.00963$, $g_{yy} = 2.00488$ and $g_{zz} = 2.00219$. For the imidazolium model these values are $g_{xx} = 2.00728$, $g_{yy} = 2.00465$ and $g_{zz} = 2.00212$. While the g_{zz} and g_{yy} values are essentially unchanged, the g_{xx} value is significantly lower for the imidazolium model. Faller et al [19] reported that for Tyr_D, at temperatures above cryogenic values, the measured *g* tensor is $g_{xx} = 2.00765$; $g_{yy} = 2.00430$; $g_{zz} = 2.00215$. At cryogenic temperatures, the g_{xx} value shifted to 2.00643. It was proposed that the cryogenic shifted g_{xx} value was due to the presence of the imidazolium form whereas the higher temperature form was due to the imidazole model. The g_{yy} and g_{zz} values did not vary as a function of temperature. The calculated g_{zz} and g_{yy} values of are generally within the accepted level of error in the experimental measurements [29] and are not changed significantly for the two forms studied. Based on previous studies on semiquinone free radicals in alcohol solutions [29], g_{xx} values are generally overestimated by 700–2000 ppm at the level of theory and basis set used here. Taking this into account the calculated values are in accord with the experimental determination. Moreover the downward shift calculated for the imidazolium model strongly supports the conclusion reached in [19] that the imidazolium form of the radical complex is trapped at

cryogenic temperatures. Heating to higher temperatures permits proton transfer from the π-nitrogen of D2-His189 to occur resulting in the imidazole form.

4. Conclusions

QM/MM calculated hyperfine and *g*-tensors for models of the Tyr_D free radical of Photosystem II show good agreement with experimental determinations. Recent small variations in proton hyperfine couplings for the three and five positions revealed by single crystal ENDOR studies are well reproduced by our modeling studies. The data further suggest that the neutral imidazole complex is formed at physiological temperatures while the imidazolium complex may be stabilized at cryogenic temperatures. Similar studies applied to the catalytically active Tyr_Z residue can contribute to further understanding of the role of the tyrosine/tyrosine radical redox couple in water oxidation by Photosystem II. Lack of experimental data for the Tyr_Z radical renders comparisons as performed here for the Tyr_D radical unlikely. However the ability to model the Tyr_D radical properties accurately as demonstrated here, will lend confidence to future calculations for the Tyr_Z radical.

References

[1] J.P. McEvoy, G.W. Brudvig, Water-splitting chemistry of photosystem II, Chem. Rev. 106 (2006) 4455–4483.
[2] G.T. Babcock, B.A. Barry, R.J. Debus, C.W. Hoganson, M. Atamian, L. Mcintosh, I. Sithole, C.F. Yocum, Water oxidation in Photosystem: 2. From radical chemistry to multielectron chemistry, Biochemistry 28 (1989) 9557–9565.
[3] P. Faller, A.W. Rutherford, R.J. Debus, Tyrosine D oxidation at cryogenic temperature in photosystem II, Biochemistry 41 (2002) 12914–12920.
[4] P. Faller, A. Boussac, R.J. Debus, K. Brettel, A.W. Rutherford, Tyrosyl radicals in photosystem II: the stable tyrosyl D and the catalytic tyrosyl Z, J. Inorg. Biochem. 86 (2001) 214.
[5] A.W. Rutherford, A. Boussac, P. Faller, The stable tyrosyl radical in Photosystem II: why D? Biochim. Biophys. Acta Bioenerg. 1655 (2004) 222–230.
[6] R.J. Debus, B.A. Barry, G.T. Babcock, L. Mcintosh, Site-directed mutagenesis identifies a tyrosine radical involved in the photosynthetic oxygen-evolving system, Proc. Natl. Acad. Sci. U. S. A. 85 (1988) 427–430.
[7] B. Loll, J. Kern, W. Saenger, A. Zouni, J. Biesiadka, Towards complete cofactor arrangement in the 3.0 angstrom resolution structure of photosystem II, Nature 438 (2005) 1040–1044.
[8] S.E.J. Rigby, J.H.A. Nugent, P.J. Omalley, The dark stable tyrosine radical of photosystem-2 studied in 3 species using Endor and Epr spectroscopies, Biochemistry 33 (1994) 1734–1742.
[9] R. Hienerwadel, A. Boussac, J. Breton, B.A. Diner, C. Berthomieu, FTIR study of TYRD and TYRZ: hydrogen bonding interactions, Photosynthesis: Mechanisms and Effects, Vols I–V, 1998, pp. 1185–1188, 4396.
[10] C. Berthomieu, R. Hienerwadel, A. Boussac, J. Breton, B.A. Diner, Hydrogen bonding of redox-active tyrosine Z of photosystem II probed by FTIR difference spectroscopy, Biochemistry 37 (1998) 10547–10554.
[11] B.A. Diner, J.A. Bautista, P.J. Nixon, C. Berthomieu, R. Hienerwadel, R.D. Britt, W.F.J. Vermaas, D.A. Chisholm, Coordination of proton and electron transfer from the redox-active tyrosine, Y-Z, of Photosystem II and examination of the electrostatic influence of oxidized tyrosine, Y-D(center dot)(H+), Phys. Chem. Chem. Phys. 6 (2004) 4844–4850.
[12] K.A. Campbell, J.M. Peloquin, B.A. Diner, X.S. Tang, D.A. Chisholm, R.D. Britt, The tau-nitrogen of D2 histidine 189 is the hydrogen bond donor to the tyrosine radical Y-D (center dot) of photosystem II, J. Am. Chem. Soc. 119 (1997) 4787–4788.
[13] R. Hienerwadel, B.A. Diner, C. Berthomieu, Molecular origin of the pH dependence of tyrosine D oxidation kinetics and radical stability in photosystem II, Biochim. Biophys. Acta-Bioenerg. 1777 (2008) 525–531.
[14] P.J. O'Malley, D. Ellson, H-1, C-13 and O-17 isotropic and anisotropic hyperfine coupling prediction for the tyrosyl radical using hybrid density functional methods, Biochim. Biophys. Acta-Bioenerg. 1320 (1997) 65–72.
[15] P.J. O'Malley, Hybrid density functional studies of the oxidation of phenol-imidazole hydrogen-bonded complexes: A model for tyrosine oxidation in oxygenic photosynthesis, J. Am. Chem. Soc. 120 (1998) 11732–11737.
[16] M. Brynda, R.D. Britt, Density functional theory calculations on the magnetic properties of the model tyrosine radical-histidine complex mimicking tyrosyl radical Y-D(center dot) in Photosystem II, Res. Chem. Intermed. 33 (2007) 863–883.
[17] R.J. Hulsebosch, J.S. vandenBrink, S.A.M. Nieuwenhuis, P. Gast, J. Raap, J. Lugtenburg, A.J. Hoff, Electronic structure of the neutral tyrosine radical in frozen solution. Selective H-2-, C-13-, and O-17-isotope labeling and EPR spectroscopy at 9 and 35 GHz, J. Am. Chem. Soc. 119 (1997) 8685–8694.
[18] S.A.M. Nieuwenhuis, R.J. Hulsebosch, J. Raap, P. Gast, J. Lugtenburg, A.J. Hoff, Structure of the Y-D tyrosine radical in photosystem II. Determination of the orientation of the phenoxyl ring by enantioselective deuteration of the methylene group, J. Am. Chem. Soc. 120 (1998) 829–830.
[19] P. Faller, C. Goussias, A.W. Rutherford, S. Un, Resolving intermediates in biological proton-coupled electron transfer: a tyrosyl radical prior to proton movement, Proc. Natl. Acad. Sci. U. S. A. 100 (2003) 8732–8735.
[20] S. Un, X.S. Tang, B.A. Diner, 245 GHz high-field EPR study of tyrosine-D degrees and tyrosine-Z degrees in mutants of photosystem II, Biochemistry 35 (1996) 679–684.
[21] R.J. Hulsebosch, J.S. vandenBrink, P. Gast, A.J. Hoff, Selectively C-13-labelled tyrosine radicals studied by electron paramagnetic resonance spectroscopy, Photosynthesis: From Light to Biosphere, Vol Ii, 1995, pp. 255–258, 988.
[22] F. Dole, B.A. Diner, C.W. Hoganson, G.T. Babcock, R.D. Britt, Determination of the electron spin density on the phenolic oxygen of the tyrosyl radical of photosystem II, J. Am. Chem. Soc. FIELD Full J. Title:J. Am. Chem. Soc. 119 (1997) 11540–11541.
[23] D.A. Force, D.W. Randall, R.D. Britt, X.S. Tang, B.A. Diner, H-2 ESE-ENDOR study of hydrogen bonding to the tyrosine radicals Y-D center dot and Y-Z center dot of photosystem II, J. Am. Chem. Soc. 117 (1995) 12643–12644.
[24] M.J. Frisch, G.W. Trucks, H.B. Schlegel, G.E. Scuseria, M.A. Robb, J.R. Cheeseman, J.J. A. Montgomery, T. Vreven, K.N. Kudin, J.C. Burant, J.M. Millam, S.S. Iyengar, J. Tomasi, V. Barone, B. Mennucci, M. Cossi, G. Scalmani, N. Rega, G. A. Petersson, H. Nakatsuji, M. Hada, M. Ehara, K. Toyota, R. Fukuda, J. Hasegawa, M. Ishida, T. Nakajima, Y. Honda, O. Kitao, H. Nakai, M. Klene, X. Li, J.E. Knox, H.P. Hratchian, J.B. Cross, C. Adamo, J. Jaramillo, R. Gomperts, R. E. Stratmann, O. Yazyev, A. J. Austin, R. Cammi, C. Pomelli, J. W. Ochterski, P. Y. Ayala, K. Morokuma, G.A. Voth, P. Salvador, J.J. Dannenberg, V.G. Zakrzewski, S. Dapprich, A.D. Daniels, M.C. Strain, O. Farkas, D.K. Malick, A.D. Rabuck, K. Raghavachari, J.B. Foresman, J.V. Ortiz, Q. Cui, A.G. Baboul, S. Clifford, J. Cioslowski, B.B. Stefanov, G. Liu, A. Liashenko, P. Piskorz, I. Komaromi, R.L. Martin, D.J. Fox, T. Keith, M.A. Al-Laham, C.Y. Peng, A. Nanayakkara, M. Challacombe, P.M.W. Gill, B. Johnson, W. Chen, M. W. Wong, C. Gonzalez and J.A. Pople. Gaussian, Inc., Pittsburgh PA 2003.
[25] T. Vreven, K.S. Byun, I. Komaromi, S. Dapprich, J.A. Montgomery, K. Morokuma, M. J. Frisch, Combining quantum mechanics methods with molecular mechanics methods in ONIOM, J. Chem. Theory Comput. 2 (2006) 815–826.
[26] P.J. O'Malley, A hybrid density functional study of the p-benzosemiquinone anion radical: the influence of hydrogen bonding on geometry and hyperfine couplings, J. Phys. Chem. 101 (1997) 6334–6338.
[27] F. Rappaport, B.A. Diner, Primary photochemistry and energetics leading to the oxidation of the (Mn)4Ca cluster and to the evolution of molecular oxygen in Photosystem II, Coord. Chem. Rev. 252 (2008) 259–272.
[28] C. Teutloff, S. Pudollek, S. Kessen, M. Broser, A. Zouni, R. Bittl, Electronic structure of the tyrosine D radical and the water-splitting complex from pulsed ENDOR spectroscopy on photosystem II single crystals, Phys. Chem. Chem. Phys. 11 (2009) 6715–6726.
[29] S.A. Mattar, Role of the solvent in computing the 1,4-benzosemiquinone *g*-tensor by the coupled-perturbed Kohn-Sham hybrid density functional method (vol 108, pg 9452, 2004), J. Phys. Chem. B 109 (2005) 3084.